JOURNAL OF BACTERIOLOGY, Sept. 1983, p. 1407–1416
0021-9193/83/091407-10$02.00/0

Vol. 155, No. 3

Regulation of *Nostoc* sp. Phycobilisome Structure by Light and Temperature

LAMONT K. ANDERSON,[1] M. CARMEN RAYNER,[2] ROBERT M. SWEET,[1]† AND FREDERICK A. EISERLING[1,2]*

Molecular Biology Institute[1] and Department of Microbiology,[2] University of California, Los Angeles, California 90024

Received 8 February 1983/Accepted 21 June 1983

Nostoc sp. strain MAC cyanobacteria were green in color when grown in white light at 30°C and contained physobilisomes that had phycoerythrin and phycocyanin in a molar ratio of 1:1. Cells grown for 4 to 5 days in green light at 30°C or white light at 39°C turned brown and contained phycoerythrin and phycocyanin in a molar ratio of greater than 2:1. In addition to the change in pigment composition, phycobilisomes from brown cells were missing a 34.5-kilodalton, rod-associated peptide that was present in green cells. The green light-induced changes were typical of the chromatic adaptation response in cyanobacteria, but the induction of a similar response by growth at 39°C was a new observation. Phycobilisomes isolated in 0.65 M phosphate buffer (pH 7) dissociate when the ionic strength or pH is decreased. Analysis of the dissociation products from *Nostoc* sp. phycobilisomes suggested that the cells contained two types of rod structures: a phycocyanin-rich structure that contained the 34.5-kilodalton peptide and a larger phycoerythrin-rich complex. Brown *Nostoc* sp. cells that lacked the 34.5-kilodalton peptide also lacked the phycocyanin-rich rod structures in their phycobilisomes. These changes in phycobilisome structure were indistinguishable between cells cultured at 39°C in white light and those cultured at 30°C in green light. A potential role is discussed for rod heterogeneity in the chromatic adaptation response.

Phycobilisomes are light-harvesting protein complexes found in cyanobacteria (10) and the chloroplasts of red algae (7, 22). These complex structures contain 10 to 15 chromophoric phycobiliproteins and nonchromophoric assembly peptides. They reside on the surface of the thylakoid membrane in direct contact with membrane-bound chlorophyll-protein complexes. The phycobiliproteins establish a chromophore network that transmits excitation energy to chlorophyll at a very high efficiency (6). The three major classes of phycobiliproteins found in *Nostoc* sp. strain MAC cyanobacteria are phycoerythrin (PE; λ_{max} = 565 nm), phycocyanin (PC; λ_{max} = 620 nm), and allophycocyanin (AP; λ_{max} = 650 nm and higher). The excitation transfer pathway for these phycobilisomes is from PE to PC to AP to chlorophyll.

Rod and core substructures have been defined for phycobilisomes from various cyanobacteria and red algae (6, 10, 17). The periphery of the phycobilisome contains five or six rodlike structures that appear to be stacks of disks. Each disk is a hexamer of phycobiliprotein protomers (α, β) in complex with a single copy of a nonchromophoric peptide (10, 11, 19). *Nostoc* sp. rods contain PE and PC and four peptides in the 29- to 35-kilodalton (kd) range that are analogous to the group II (26), linker (19), and accessory (21) peptides described for other phycobilisomes. We call these four peptides rod-associated peptides (RAPs). The *Nostoc* sp. phycobilisome core appears as a triangular packet of disks viewed face-on (13). It contains all of the AP-type biliproteins and other core-associated peptides. These include a 95-kd polypeptide that anchors the structure to the membrane (32) and may be a terminal energy acceptor (20) and some 45- to 50-kd AP-associated peptides (32). The spatial arrangement of the phycobiliproteins reflects the excitation transfer pathway within the phycobilisome. The outer portion of the rods contains PE, whereas the inner region contains PC that is connected to the AP-containing core (5, 17, 27).

Phycobilisomes can be isolated in concentrated phosphate salt solutions and separated from cell debris by sedimentation (7, 28). Hydrophobic interactions that stabilize phycobilisome structure (33) are disrupted when the salt concentration is decreased from 0.65 M NaK-PO_4

†Present address: Brookhaven National Laboratories, Upton, NY 11973.

(see Materials and Methods). Phycobilisome dissociation causes loss of the characteristic 680-nm fluorescence emission and can produce stable substructures the size of which is directly related to the ionic strength and the pH of the solution. We dissociated *Nostoc* sp. phycobilisomes at pH 7 or 5 in 0.3 M NaK-PO_4 to generate rod substructures and to provide a means of analyzing changes in phycobilisome rod structure that are induced by different growth conditions.

MATERIALS AND METHODS

Cyanobacteria and culture conditions. *Nostoc* sp. strain MAC was obtained from E. Gantt (Smithsonian Radiation Biology Laboratory, Rockville, Md.) and is the same strain used in previous studies (13, 16). Cells were grown in medium BG-11 (23), with continuous agitation and bubbling of 1% CO_2 in air, in three environments: warm white fluorescent light at 30°C (30W cells), warm white fluorescent light at 39°C (39W cells), and green light (Westinghouse F15T8/G) at 30°C (30G cells). The light intensity for the 30W and 39W cultures was 10^{-2} μE/cm^2 per s. The light intensity for the 30G cells was 1.2×10^{-2} μE/cm^2 per s.

Phycobilisome isolation. *Nostoc* sp. cells were grown to 0.8 to 1 g (wet weight) per liter and harvested by filtration through Miracloth. Filaments were resuspended to 0.1 g/ml in 0.65 M NaK-PO_4 (pH 7). All NaK-PO_4 buffers were made by titration of equimolar solutions of NaH_2PO_4 and K_2HPO_4 to the desired pH. The cells were broken by two passages through a French pressure cell at 14,000 lb/in^2. Triton X-100 was added at 2% (vol/vol), and the mixture was incubated at 22°C with occasional agitation for 30 min. Cell debris was removed by centrifugation at 27,000 × *g* for 30 min at 20°C, and 4 to 5 ml of the supernatant was loaded onto sucrose step gradients of 0.25 M (5 ml), 0.5 M (5 ml), 0.75 M (6 ml), 1.0 M (6 ml), 1.5 M (8 ml), and 2.0 M (5 ml) sucrose in 0.65 M NaK-PO_4 (pH 7). Gradients were centrifuged in a Beckman VTi 50 rotor at 50,000 rpm and 20°C for 90 min. The phycobilisomes were recovered from the 1.5 M sucrose region of the gradient and dialyzed against 0.65 M NaK-Po_4 (pH 7) at 20°C for 2 h. Ammonium sulfate (750 g in 1 liter of water) was added dropwise (1.3 volume to 2.3 volumes of phycobilisomes) at room temperature with gentle stirring, and the precipitated phycobilisomes were collected by sedimentation at 12,000 × *g* for 30 min at 20°C. The pellet was resuspended in 0.65 M NaK-PO_4–1.0 M sucrose (pH 7) to a total phycobiliprotein concentration of approximately 10 mg/ml and stored at −20°C until needed.

Absorption and fluorescence measurements. Absorbances were measured in a Beckman model 25 spectrophotometer at 565 nm (PE), 620 nm (PC), and 650 nm (AP). Fluorescence emission spectra were measured with an Aminco SPF-500 spectrofluorimeter interfaced to a Hewlett-Packard 9815A/S computer which corrected the signal for the decrease in photomultiplier tube response at long wavelengths. Samples were diluted to an absorbance of 0.04 for the most abundant phycobiliprotein. Emission spectra were obtained for excitation at 500 or 600 nm with slit widths of 5 nm for excitation and 2 nm for emission.

Estimation of phycobiliprotein concentrations. Phycobiliprotein concentrations were estimated from absorbances by the equations of Bryant et al. (5) and assuming α + β protomeric masses for PE, PC, and AP of 39.8, 36.9, and 33.8 kd, respectively (based on relative mobility in 4 to 20% acrylamide gradient sodium dodecyl sulfate [SDS] acrylamide gel). Absorbances of dissociated phycobilisomes (see Fig. 2) were read directly from the gradient fractions. Absorbances for molar ratio determinations (see Tables 1 and 2) were obtained after dilution with water to 50 mM PO_4.

SDS-acrylamide gel electrophoresis. Improved resolution of biliproteins and RAPs occurred with a 4 to 20% polyacrylamide linear gradient made from a stock solution of 30% acrylamide–1.6% bisacrylamide and a stacking gel made from the same stock solution. The discontinuous buffer system of Laemmli (18) was used, except the amount of Tris in the running gel was doubled. Although this gel system clearly separates the 34.5- and 34-kd RAPs, they are transposed relative to mobilities seen in other gel systems (13, 16). A similar situation has been observed for the gene 48 product of bacteriophage T5, where gel composition causes anomalous migration of this protein (1, 15). The RAPs from *Nostoc* sp. phycobilisomes will be referred to by the published masses (13) to avoid confusion (see Fig. 1). Samples were prepared for electrophoresis by precipitation with 4 volumes of cold 10% trichloroacetic acid, centrifugation at 12,000 × *g* for 15 min, and resuspension in the desired volume of 1× Laemmli sample buffer (18). Samples were heated at 100°C for 2 min before application. Electrophoresis was performed at 100 V for 14 h, after which the gels were fixed in 25% isopropanol–10% acetic acid for at least 4 h. Gels were stained in 25% isopropanol–10% acetic acid–0.04% Coomassie blue R-250 and destained in 10% acetic acid.

Dissociation analysis on 0.3 M PO_4 sucrose sedimentation gradients. Frozen solutions of phycobilisomes at a total phycobiliprotein concentration of ca. 10 mg/ml were thawed, diluted to 5 mg/ml with 0.3 M NaK-PO_4 at the desired pH (7 or 5), and dialyzed for 2 h at 20°C against 1 liter of 0.3 M NaK-PO_4 (pH 7 or 5). A 0.5-ml volume of the dialyzed material was loaded onto a 39-ml 0.25 to 1.5 M sucrose linear gradient in 0.3 M NaK-PO_4 (pH 7 or 5). A 0.5-ml solution of sedimentation marker proteins was loaded on identical salt gradients at pH 7 or 5. The marker protein solution contained the following in sufficient quantities to produce an independent absorbance of 2.5 at the indicated wavelength: *Anabaena variabilis* AP trimers at 650 nm (6S and 103 kd); *Porphyridium cruentum* B-PE hexamers (B-PE) at 550 nm (12.5S and 263 kd); and *Salmonella typhimurium* glutamine synthetase (GS) at 280 nm (20.3S and 592 kd). This protein mixture was dialyzed for 2 h against the same buffer as that used for phycobilisome dissociation. Gradients were centrifuged at 50,000 rpm in a Beckman VTi 50 rotor for 5 h at 20°C. Fractions of 1.1 ml were collected through a needle introduced into the bottom of the tube. Absorbance was measured at specific wavelengths for each fraction to generate the phycobiliprotein concentration profiles from the gradients. The dissociation patterns for 0.3 M NaK-PO_4 (pH 7) did not change over the phycobiliprotein concentration range of 2 to 8 mg/ml. Selected fractions were used immediately after frac-

TABLE 1. Molar ratios of phycobiliproteins in phycobilisome preparations

Phycobilisome type	Molar ratio		
	PE/PC	PC/AP	PE/AP
30W	1:1	0.6:1	0.6:1
39W	2.3:1	0.4:1	0.9:1
30G	2.4:1	0.4:1	0.9:1
30G (3 days posttransfer)	1.6:1	0.5:1	0.8:1

tionation for fluorescence measurements, molar ratio calculations, electron microscopy, and SDS-acrylamide gel electrophoresis.

Electron microscopy. Material for microscopy was freshly diluted to a total phycobiliprotein concentration of 0.05 to 0.2 mg/ml with 0.65 M NaK-PO_4–0.5 M sucrose (pH 7 or 5). Carbon was evaporated onto freshly cleaved mica, and with the aid of a microscope slide translation stage, the carbon film was floated onto the sample surface without completely detaching the film from the mica. The carbon-bearing mica was then transferred to freshly made 1% glutaraldehyde in 0.65 M NaK-PO_4–0.5 M sucrose (pH 7 or 5). After 5 min, the carbon film was transferred to distilled water for 8 min. After the wash, 400-mesh copper grids were placed upon the carbon film, and if the film was intact, it was detached from the mica with forceps. The grid was then transferred briefly to 0.5% uranyl acetate and removed, and excess stain was absorbed with filter paper. All electron microscopy was performed with a JEOL 100B transmission electron microscope.

Reagents and chemicals. Ultra-pure ammonium sulfate and enzyme grade sucrose were from Schwarz/Mann, Orangeburg, N.Y. The acrylamide and bisacrylamide were from Eastman Kodak Co., Rochester, N.Y. All other chemicals were reagent grade.

RESULTS

When *Nostoc* sp. cultures were transferred from 30°C, white light, to 39°C, white light, or 30°C, green light, an adaptation process was initiated, and the cells changed from green to brown in color. Although a color difference between cultures was visually evident after day 1, the complete transition required 4 to 5 days. Isolated phycobilisomes from all three growth conditions showed that the cellular color transition from green to brown was accompanied by an increase in the PE/PC molar ratio from 1:1 to greater than 2:1 (Table 1).

Electropherograms of phycobilisomes from 30W, 39W, and 30G cells are shown in Fig. 1. When *Nostoc* sp. cells were cultured in white light at 30°C, phycobilisomes had a PE/PC molar ratio of 1:1 and contained four RAPs that were identified by their apparent masses (34.5, 34, 32, and 29 kd) (13). The absence of the 34.5-kd RAP in 39W and 30G cells was accompanied by an

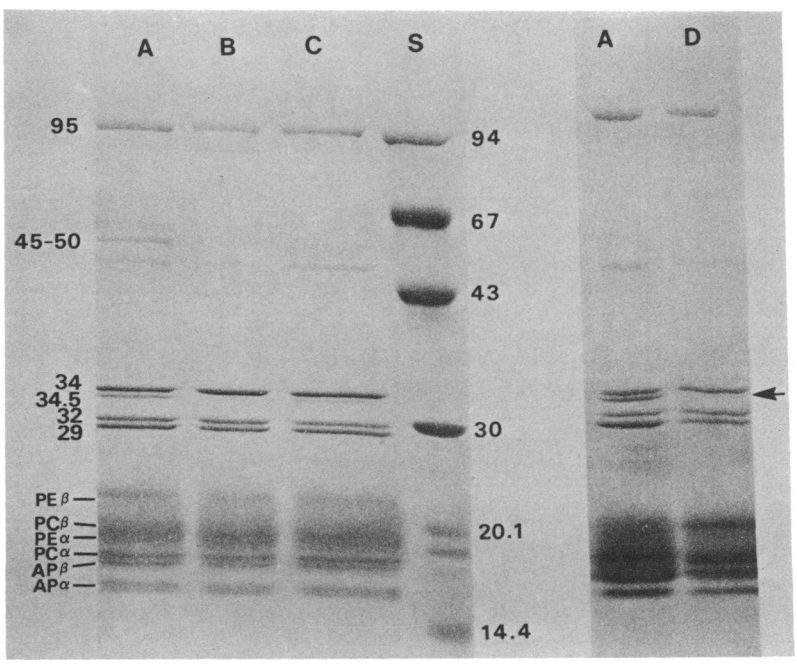

FIG. 1. SDS-acrylamide gels of phycobilisomes from *Nostoc* sp. cells grown under different conditions. Lane A, white light, 30°C; lane B, white light, 39°C; lane C, green light, 30°C, partially adapted (see text); lane D, green light, 30°C, fully adapted. S, Molecular weight standards: phosphorylase b, bovine serum albumin, ovalbumin, carbonic anhydrase, soybean trypsin inhibitor, alpha-lactalbumin. Lanes A and D to the right of the standards were run on a 4 to 25% linear gradient SDS-acrylamide gel made from stock with 30% acrylamide–2% bisacrylamide. A total of 15 to 20 μg of total phycobiliproteins was loaded on the gels. The arrow indicates the position of the 34.5-kd RAP.

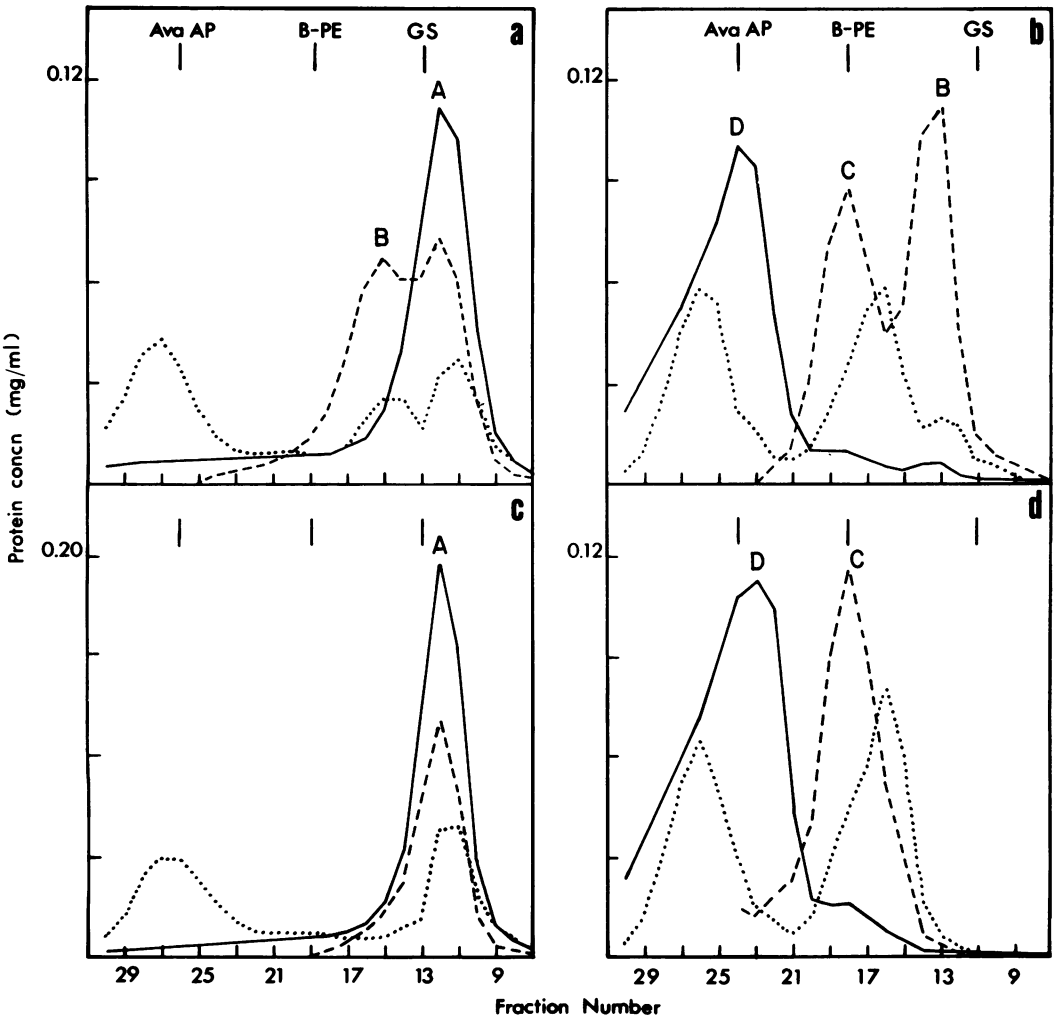

FIG. 2. Concentration of individual phycobiliproteins in 1.1-ml fractions of dissociation gradients. (a) 30W phycobilisomes at 0.3 M NaK-PO_4 (pH 7); (b) 30W phycobilisomes at 0.3 M PO_4 (pH 5); (c) 39W phycobilisomes at 0.3 M NaK-PO_4 (pH 7); (d) 39W phycobilisomes at 0.3 M NaK-PO_4 (pH 5). The top of the gradients is at the left of figure. ———, PE; ----------, PC, ·····, AP. Fractions which contained the maximum absorbance of the sedimentation marker proteins are indicated at the top of the figure. The letters A through D are labels for species described in the text.

increase in the amount of PE relative to phycobilisomes from 30W cells. The disappearance of the 34.5 kd RAP from *Nostoc* sp. cells grown in green light has been previously observed (16). The decrease or loss of RAPs upon chromatic adaptation has been demonstrated in other cyanobacteria and has helped establish relationships between phycobiliproteins and RAPs (8, 10, 26). Our analysis of dissociated phycobilisomes that contained the 34.5-kd RAP (from 30W cells) was augmented by a comparison with dissociation patterns of phycobilisomes that lacked the 34.5-kd RAP (from 39W or 30G cells).

Dissociation patterns of phycobilisomes. The distribution of dissociation products throughout a sedimentation gradient can be shown as a graph of phycobiliprotein concentrations plotted against the distance migrated through the gradient. Such a dissociation pattern for 30W phycobilisomes at pH 7 is shown in Fig. 2a. Approximately half of the AP appeared in the region of the gradient defined by the trimeric AP marker protein. The remainder of the AP was distributed in two peaks in the lower part of the gradient with the rod phycobiliproteins PC and PE. The rod proteins were separated into two peaks. Species A sedimented ahead of the GS marker and species B ran behind the peak GS fraction,

but in front of the B-PE marker. Species A (PE rich) contained more than 70% of the PE, 30 to 40% of the PC, and 30% of the AP. Species B (PC rich) was composed of 50% of the PC and also contained 10 to 20% of the PE and 20% of the total AP.

The pH 5 dissociation pattern of phycobilisomes from 30W cells is shown in Fig. 2b. Comparison of the gradient position of the heaviest PC material to the sedimentation markers B-PE and GS indicated a sedimentation rate similar to that observed for species B in the pH 7 gradient. This material was also labeled B. A PC species that sedimented slightly ahead of the B-PE marker was labeled C, and all of the PE was found in the region of the gradient marked by AP trimers, labeled D. The dissociation pattern of core material (AP) at pH 5 revealed two separate components which appeared to sediment independently of the rod proteins.

After dialysis to 0.3 M PO_4 (pH 7 and 5), 39W and 30G phycobilisomes yielded the dissociation patterns shown in Fig. 2c and d. Although only data from 39W phycobilisomes are shown, the dissociation patterns for the 39W and 30G phycobilisomes were indistinguishable. Comparison of these gradient profiles with the profiles from 30W cells showed that 39W or 30G phycobilisomes did not yield species B material after dissociation at either pH. All other aspects of the 39W or 30G dissociation patterns were similar to the 30W results.

Electron microscopy of dissociation products. Electron micrographs in Fig. 3a and b show the structures in species A and B from the pH 7 gradient of 30W phycobilisomes. Species A (see arrows) shows a stack of three disks that resemble the rod substructures observed on intact *Nostoc* sp. phycobilisomes (13). Species B contained stacks of double disks seen edge-on (Fig. 3b; see arrows) or face-on. Electron micrographs (Fig. 3c and d) of PC species from the pH 5 gradient of 30W phycobilisomes showed double- and single-disk structures for species B and C, respectively. The pH 5 B sample contained fewer edge-on views of the stacked double-disk structures seen in the pH 7 species B and often showed a face-on view of two disks attacned side by side (see arrows). Material from zone C appeared as single disks, often with stain penetration in the middle. Micrographs of species A (pH 7) and species C (pH 5) from 39W or 30G phycobilisomes were similar to the analogous micrographs shown in Fig. 3. Trimers from cyanobacteria are difficult to visualize in the electron microscope (4), and no data for species D were obtained.

Polypeptide composition of dissociation products. Figures 4a and b show SDS-acrylamide gel analyses of the dissociation gradients from Fig.

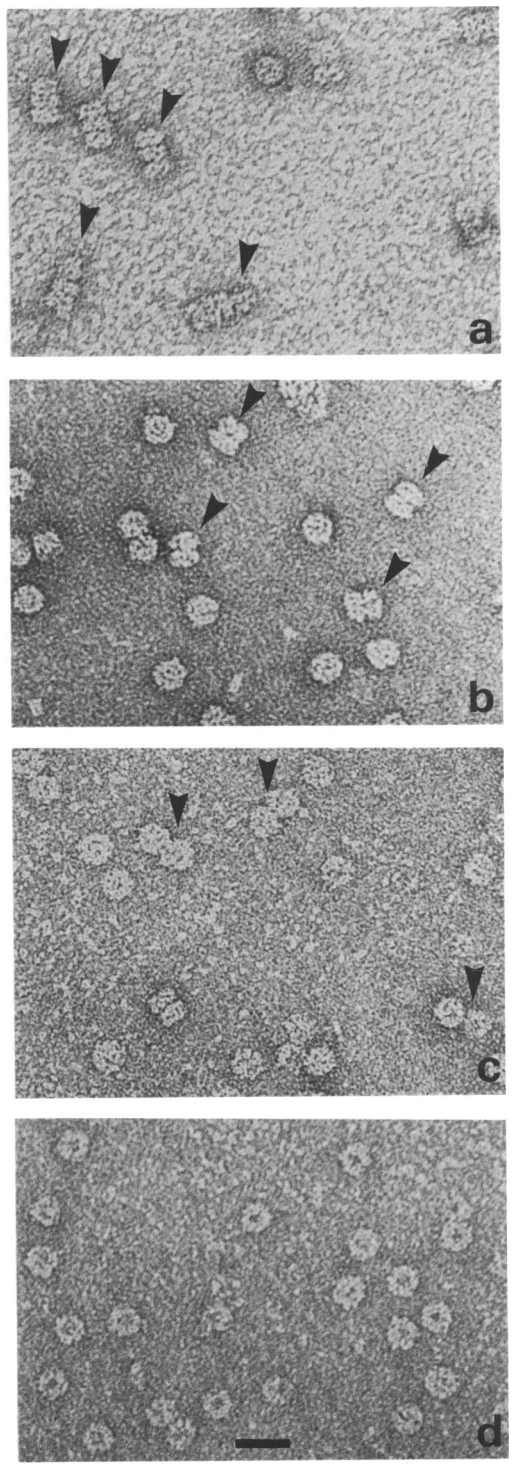

FIG. 3. Electron micrographs of dissociation products. (a) Species A from Fig. 2a; (b) species B from Fig. 2a; (c) species B from Fig. 2b; (d) species C from Fig. 2b (bar, 20 nm). Magnification, ×337,000.

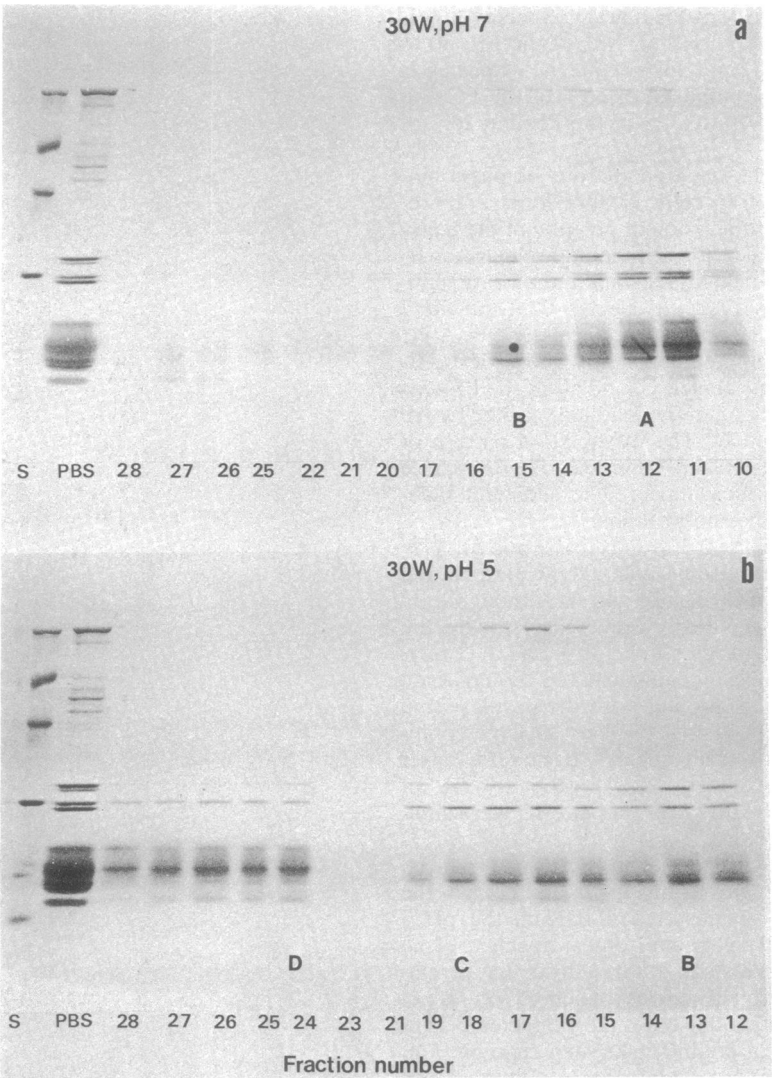

FIG. 4. SDS-acrylamide gels of fractions from 30W phycobilisome dissociation gradients. (a) Fractions from 0.3 M NaK-PO_4 (pH 7) gradient (Fig. 2a); (b) fractions from 0.3 M NaK-PO_4 (pH 5) gradient (Fig. 2b). Molecular weight standards (S) are the same as those listed in the legend to Fig. 1. PBS, Whole phycobilisomes from 30W cells. Identical volumes of prepared gradient fractions were loaded on the gels to give a maximum of 20 to 25 μg of phycobiliproteins.

2a and b. Maximum Coomassie staining for the RAPs or core-associated peptides was consistently observed in fractions of maximal phycobiliprotein concentration. Such data imply a direct structural affiliation between phycobiliproteins and the RAPs or core-associated peptides for the following reasons: the RAPs from *Synechococcus* sp. 6301 are required to assemble PC into stacked-disk rod structures (10, 19); RAP-induced changes in spectral properties of *Synechococcus* sp. 6301 PC are important for the establishment of the highly efficient excitation transfer system of the phycobilisome (10); isolated RAPs are insoluble in the absence of high concentrations of urea or other denaturing agents (19); and RAP- and core-associated peptide–biliprotein complexes from *Nostoc* sp. were isolated with harsher treatments than those employed in these experiments (13, 32).

In the pH 7 dissociation gradient, three of the RAPs—the 34-, 32-, and 29-kd polypeptides—cosedimented with the PE-rich A species (fraction 12). In the PC-rich B zone of the pH 7 gradient, the 34- and 32-kd peptides decreased in staining intensity, whereas the 29-kd peptide remained constant and the 34.5-kd peptide ap-

TABLE 2. Data for dissociation products of *Nostoc* sp. phycobilisomes

Species	Growth conditions[a]	PE/PC molar ratio	RAP with species	Structural appearance
pH 7				
A	30W	1.8:1	34, 32, 29	3-disk rods
B	30W	0.2:1	34.5, 29	2-disk rods
A	39W	1.9:1	34, 32, 29	3-disk rods
A	30G	1.8:1	34, 32, 29	3-disk rods
pH 5				
B	30W	0.06:1	34.5, 29	2 disks[b]
C	30W, 39W	0.1:1	34, 29	Single disks
D	30W, 39W	21:1	34, 32	Not observed

[a] Data are for phycobilisomes from cells grown in the conditions indicated and defined in the text.
[b] Appear as face-on view of two disks attached side by side.

peared in this region (fraction 15). The 95- and 45- to 50-kd peptides and AP were also present in A and B regions of the pH 7 gradient. Electropherograms of pH 5 dissociated 30W phycobilisomes (Fig. 4b) showed that the B region (fraction 13) contained only 34.5- and 29-kd RAPs, the two RAPs found with the B sample from the pH 7 gradient. Species C contained the 34- and 29-kd peptides as well as PC (fraction 18). The PE component, D, had the 32-kd peptide and some traces of the 34-kd peptide (fraction 24). SDS-acrylamide gel analysis of the pH 7 and 5 gradients for 39W or 30G phycobilisomes differed from that of the 30W phycobilisomes only in the absence of those polypeptides associated with species B in pH 7 and 5 gradients.

The disposition of the RAPs throughout the pH 5 gradient implied structural associations between the 32-kd peptide and PE and between the 34.5-, 34-, and 29-kd peptides and PC. The material from peak B had the same major components (PC subunits, 34.5- and 29-kd RAPs) in both pH 5 and 7 gradients, suggesting that the decrease in pH destabilized the rods of species A, which dissociated into PC and PE species C and D (Fig. 2b). The peptides that cosedimented with AP in both gradients (95- and 45- to 50-kd polypeptides) were probably associated with the AP, since they have been isolated from *Nostoc* sp. in complex with AP (32).

The compositional and structural data for the rod-related dissociation products are summarized in Table 2.

Fluorescence energy transfer of dissociation products. Maximal fluorescence of species A was at 652 nm, with a smaller maximum at 580 nm (Fig. 5a), indicating that the majority of the PE in this material is energetically coupled to PC. The 652-nm emission was interpreted as red-shifted PC fluorescence characteristic of PC in complex with RAPs (10, 19) and has been observed in *Nostoc* sp. rod preparations in another laboratory (13). The maximum fluorescence for species B (pH 7) occurred at 652 nm, although substantial fluorescence was also observed at 580 nm (Fig. 5a). Excitation of peak B materials with 600-nm light yielded a 652-nm emission, but at a ca. 10-fold-higher relative

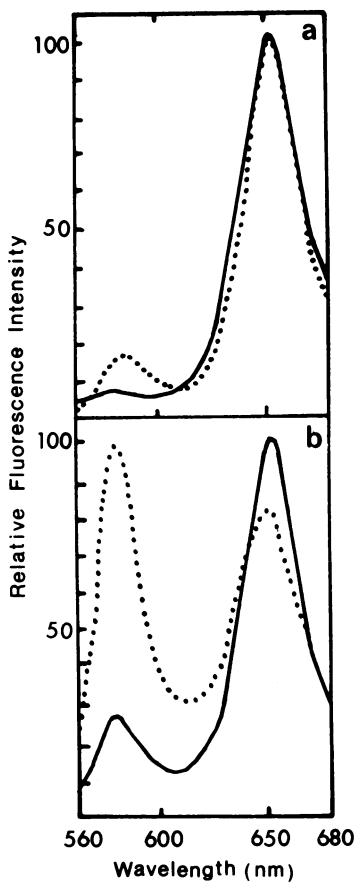

FIG. 5. Fluorescence energy transfer of dissociation products. (a) Samples from 0.3 M NaK-PO_4 (pH 7) gradient: ———, species A; ·····, species B. (b) Samples from 0.3 M NaK-PO_4 (pH 5) gradient: ———, species B; ·····, species C. The long-wavelength maxima are at 652 nm.

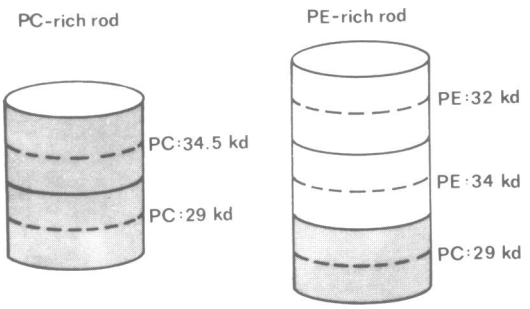

FIG. 6. Rod heterogeneity in *Nostoc* sp. phycobilisomes. Disk boundaries are indicated by solid lines, and each represents a hexamer of the specified phycobiliprotein with a single copy of a rod-associated protein. The dotted lines indicate the trimer divisions. The core binding sites are at the bottom of these structures.

TABLE 3. Mass estimations of 30W phycobilisome dissociation products in pH 7 and 5 gradients

Protein or dissociation product	M(obs) (kd)[a]	X^b		M(calc) (kd)[c]	
		pH 7	pH 5	pH 7	pH 5
GS	592	0.6486	0.6944	591	616
B-PE	263	0.4864	0.5000	264	241
AvaAP	103	0.2973	0.3333	103	108
Species A	790	0.6757		680	
Species B	510	0.5946	0.6389	450	470

[a] Marker protein observed mass values [M(obs)] were determined as described in the text. The observed mass values for species A and B were calculated assuming the rod compositions shown in Fig. 6.

[b] $X = (N - n)/N$, where N = total number of fractions in the gradient and n = peak fraction number for the species. The data were fit by least squares to the equation $\ln M = aX + b$. For pH 7 gradients: $a = 5.414$, $b = 9.780$; pH 5 gradients: $a = 5.256$, $b = 9.688$.

[c] Calculated mass values [M(calc)] were determined by use of these parameters and the X values listed in the equation in footnote *b*.

fluorescence intensity (data not shown), indicating that very little, if any, PE is coupled to PC in this sample. The AP in both of these samples was not functionally associated with rod components in either species, as indicated by the absence of a 680-nm fluorescence.

When excited at 500 nm, both B and C material from the pH 5 gradient had large emission signals at 652 nm (Fig. 5b). Regardless of differences in dissociation states between pH 5 and 7, a major portion of the fluorescence in B and C samples (pH 5) was the result of a PC component with a maximum of 652 nm. Both samples demonstrated significant 580-nm emission signals, indicating the presence of PE that is not coupled to PC.

DISCUSSION

Our characterization of the PE- and PC-rich dissociation products from 30W phycobilisomes suggested the existence of two classes of rod structure in *Nostoc* sp. Partially dissociated 39W and 30G phycobilisomes lacked the PC-rich rod component. The PC-rich material thus represents a second class of rod structure if the PE-rich rods are identical and are attached directly to the core in 39W, 30G, and 30W phycobilisomes.

We propose that the PE-rich rods consist of two PE hexamers and one PC hexamer. The 29-kd RAP is needed to join PE-rich rods to cores (13) and is placed at the PC terminus, where the core binding site is located. Since the 32-kd peptide is always associated with a PE complex, it must be localized at the PE terminus of the three-disk stack. The 34-kd peptide is found with both PE and PC at pH 5 and is probably a connector between PE and PC (Fig. 6). The PC-rich rods have virtually no naturally bound PE, based on SDS-acrylamide gels and fluorescence data. Because these particles contain two hexameric disks and the 29- and 34.5-kd RAPs and because the 29-kd RAP is the connection to the core, we conclude the structure has two PC hexamers, the outer one complexed with the 34.5-kd RAP and the inner one associated with the 29-kd RAP (Fig. 6).

Table 3 shows further data supporting this model. The approximate masses of the dissociation products were estimated from their positions in sucrose gradients relative to the marker proteins. AP, B-PE, and GS are stable as trimers, hexamers, and dodecamers, respectively, at both pH 7 and 5 (4, 9, 12, 14). Three M_r values of 240, 265, and 280 kd have been obtained for B-PE by different methods (7, 12). We assumed a minimal mass of 263 kd for B-PE hexamers because the β subunit of B-PE, with three chromophores, is at least as large as the sequenced PC β subunit of *Mastigocladus laminosus*, with two chromophores (24). Since the α and β subunits of B-PE are equivalent in mass (7, 12), a subunit mass of 19.4 kd (the PC β mass) was assumed. A mass of 30 kd for the γ subunit of B-PE results in the 263-kd value for $(\alpha, \beta)_6\gamma$ used in Table 3. The sum of the masses of the proteins in the PE-rich rod model yields an approximate mass of 790 kd, whereas the value calculated from the sedimentation data is 680 kd. The difference between the expected and the observed masses is the equivalent of a phycobiliprotein trimer. Given the uncertainty in making the mass estimates, a difference of one trimer for a 3-hexamer structure does not contradict the model. The expected mass of the PC-rich rods is 510 kd versus the calculated values of 450 kd

(pH 7) or 470 kd (pH 5), supporting the model for the PC-rich rods.

The independent structural roles for the two types of rods is supported by the fluorescence emission spectra. The 652-nm emission for both rod species suggests similar functions in the excitation transfer process. In *Synechococcus* 6301, the longer wavelength PC fluorescence (652 versus 646 nm) is the result of interaction between PC and the 27-kd RAP at the rod-core interface. The smallest RAP is located at the interface for rod and core in *Synechococcus* sp. 6301 (19), *Synechocystis* sp. 6701 (8), *A. variabilis* (29, 30), and *Nostoc* sp. (13). After dissociation at pH 5, we found the 652-nm emission in the stable PC-rich structure (species B) and the PC dissociation product (species C) of the PE-rich rods. The presence of the 29-kd RAP and the 652-nm fluorescence at pH 7 indicates that each structure contains PC-RAP complexes capable of transferring excitation directly to the phycobilisome core.

The PE- and PC-rich rods described here are remarkably similar in structure, composition, and function to two complexes isolated from *Nostoc* sp. by Glick and Zilinskas (13) and Zilinskas (31), using different methods. These authors performed reconstitution experiments that suggested rod heterogeneity. Our physical and biochemical data support this suggestion.

This paper documents the independent transitions that temperature and light quality induce in the phycobilisome population between a PC-enriched, rod-heterogenous state and a PE-enriched, rod-uniform state. The PE enrichment that occurs in green light is characteristic of chromatic adaptation in cyanobacteria (3, 5, 25). Chromatic adaptation optimizes cellular pigment content for the quality of light in which the organism grows. Three categories of adaptation have been described (25). Group I cyanobacteria do not adapt. Group II organisms control PE levels by adjusting the amount of PE-RAP complexes at the free ends of the rod structures, but do not adjust the amount of PC (5, 8, 19). Group III cyanobacteria control both PE and PC in a complementary process, increasing PE and decreasing PC in green light and reversing this response in red light. A second pair of inducible PC subunits is the probable means of regulating PC levels in most but not all group III organisms (2, 3). How these extra PC subunits are accommodated within the phycobilisome structure is not yet known.

Nostoc sp. strain MAC lacks the inducible PC subunits and has been classified as a group II adapter (16). Our data on isolated phycobilisomes suggest that *Nostoc* sp. cells can vary the amount of PC relative to PE and AP (Table 1) and might be considered a group III organism on the basis of changes in the overall levels of PE and PC in response to light quality. The adaptation response in *Nostoc* sp. is effected by controlling the relative levels of the two types of rod structures in the phycobilisome population. Cells at an intermediate stage of green light adaptation had decreased levels of the 34.5-kd peptide (Fig. 1, track C), an intermediate PE/PC molar ratio (Table 1), and an intermediate amount of the PC-rich rods (data not shown). The proposed regulation of PE and PC in *Nostoc* sp. by varying the levels of the PE- and PC-rich rods could only result in an apparent complementary adaptation response, supporting a group III designation.

The absence of the 34.5-kd RAP from whole-cell extracts of 39W and 30G cells (unpublished observation) implies that expression of the gene for the 34.5-kd peptide is regulated independently by light and temperature. Control of PC and PE production may be coordinated with that of RAPs to achieve proper stoichiometery. Regulation of gene expression by light quality is an important adaptive response in many cyanobacteria (3, 16, 25). Our new observation that a similar response can be elicited by changes in temperature may provide a new approach to investigating the adaptation phenomenon.

ACKNOWLEDGMENTS

This work was supported by National Science Foundation grant PCM 80-21363 (to F.A.E.) and Public Health Service grant GM27076 from the National Institutes of Health (to R.M.S.). L.K.A. was supported by Public Health Service National Research Service Award GM07185 from the National Institutes of Health.

We thank John Rayner for performing the spectrofluorimeter measurements. The *S. typhimurium* GS was a gift from Cheryl Janson.

ADDENDUM

After this paper was submitted, a report by Zilinskas and Howell (Plant Physiol. **71**:379–387, 1983) described the affect of pink light on phycobilisome structure in *Nostoc* sp. strain MAC. Their results, obtained by using 37°C cultures in white light, were identical to ours for 39W phycobilisomes. They induced adaptation with pink light at 37°C and obtained phycobilisomes similar to our 30W phycobilisomes, thus confirming the idea that phycobilisome structure in *Nostoc* sp. is regulated by light and temperature conditions during growth.

LITERATURE CITED

1. **Berget, P. B., and H. R. Warner.** 1975. Identification of P48 and P54 as components of bacteriophage T4 baseplates. J. Virol. **16**:1669–1677.
2. **Bryant, D. A.** 1981. The photoregulated expression of multiple phycocyanin species. Eur. J. Biochem. **119**:425–429.
3. **Bryant, D. A., and G. Cohen-Bazire.** 1981. Effects of chromatic illumination on cyanobacterial phycobilisomes. Eur. J. Biochem. **119**:415–424.
4. **Bryant, D. A., A. N. Glazer, and F. A. Eiserling.** 1976. Characterization and structural properties of the major biliproteins of *Anabaena* sp. Arch. Microbiol. **110**:61–75.

5. **Bryant, D. A., G. Guglielmi, N. Tandeau de Marsac, A. Castets, and G. Cohen-Bazire.** 1979. The structure of cyanobacterial phycobilisomes: a model. Arch. Microbiol. **123**:113–127.
6. **Emerson, R., and C. M. Lewis.** 1942. The photosynthetic efficiency of phycocyanin in *Chroococcus*, and the problem of carotenoid participation in photosynthesis. J. Gen. Physiol. **25**:579–595.
7. **Gantt, E., and C. A. Lipshultz.** 1974. Phycobilisomes from *Porphyridium cruentum*: pigment analysis. Biochemistry **13**:2960–2966.
8. **Gingrich, J. C., R. C. Williams, and A. N. Glazer.** 1982. Rod substructures in cyanobacterial phycobilisomes: phycoerythrin assembly in *Synechocystis* 6701 phycobilisomes. J. Cell Biol. **95**:170–178.
9. **Ginsburg, A.** 1972. Glutamine synthetase of *E. coli*: some physical and chemical properties. Adv. Protein Chem. **26**:1–79.
10. **Glazer, A. N.** 1982. Phycobilisomes: structure and dynamics. Annu. Rev. Microbiol. **36**:173–198.
11. **Glazer, A. N., and S. Fang.** 1973. Formation of hybrid proteins from the alpha and beta subunits of phycocyanins of unicellular and filamentous blue-green algae. J. Biol. Chem. **248**:663–671.
12. **Glazer, A. N., and C. S. Hixson.** 1977. Subunit structure and chromophore composition of the Rhodophytan phycoerythrins. J. Biol. Chem. **252**:32–42.
13. **Glick, R. E., and B. A. Zilinskas.** 1982. Role of the colorless polypeptides in phycobilisome reconstitution from separated phycobiliproteins. Plant Physiol. **69**:991–997.
14. **Hattori, A., and Y. Fujita.** 1958. Crystalline phycobilin chromoproteins obtained from a blue-green algae, *Tolypothrix tenuis*. J. Biochem. (Tokyo) **46**:633–644.
15. **Kikuchi, Y., and J. King.** 1975. Genetic control of bacteriophage T4 baseplate morphogenesis. II. Mutants unable to form the central part of the baseplate. J. Mol. Biol. **99**:673–694.
16. **Kipe-Nolt, J. A., S. E. Edwards, Jr., and D. A. Bryant.** 1982. Growth and chromatic adaptation of *Nostoc* sp. strain MAC and the pigment mutant R-MAC. Plant Physiol. **70**:1549–1553.
17. **Koller, K.-P., W. Wehrmeyer, and E. Morschel.** 1978. Biliprotein assembly in the disc-shaped phycobilisomes of *Rhodella violacea*. Eur. J. Biochem. **91**:57–63.
18. **Laemmli, U. K.** 1970. Cleavage of structural proteins during the assembly of the head of bacteriophage T4. Nature (London) **227**:680–685.
19. **Lundell, D. J., R. C. Williams, and A. N. Glazer.** 1981. Molecular architecture of a light-harvesting antenna: in vitro assembly of the rod substructures of *Synechococcus* 6301 phycobilisomes. J. Biol. Chem. **256**:3580–3592.
20. **Lundell, D. J., G. Yamanaka, and A. N. Glazer.** 1981. A terminal energy acceptor of the phycobilisome: the 75,000-dalton polypeptide of *Synechococcus* 6301 phycobilisomes—a new biliprotein. J. Cell Biol. **91**:315–319.
21. **Morschel, E.** 1982. Accessory polypeptides in phycobilisomes of red algae and cyanobacteria. Planta **154**:251–258.
22. **Redlinger, T., and E. Gantt.** 1981. Phycobilisome structure of *Porphyridium cruentum*. Plant Physiol. **68**:1375–1379.
23. **Rippka, R., J. Deruelles, J. B. Waterbury, M. Herdman, and R. Y. Stanier.** 1979. Generic assignments, strain histories, and properties of pure cultures of cyanobacteria. J. Gen. Microbiol. **111**:1–61.
24. **Sidler, W., P. Fuglistaller, J. Gysi, E. Isker, and H. Zuber.** 1981. The complete amino acid sequence of allophycocyanin from the cyanobacterium *Mastigocladus laminosus*, secondary structure predictions and comparison with C-phycocyanin and with fragments of C-phycoerythrin and phycoerythrocyanin, p. 583–594. *In* G. Akoyunoglou (ed.), Photosynthesis III. Structure and molecular organization of the photosynthetic apparatus. Balaban International Science Services, Philadelphia, Pa.
25. **Tandeau de Marsac, N.** 1977. Occurrence and nature of chromatic adaptation in cyanobacteria. J. Bacteriol. **130**:82–91.
26. **Tandeau de Marsac, N., and G. Cohen-Bazire.** 1977. Molecular composition of cyanobacterial phycobilisomes. Proc. Natl. Acad. Sci. U.S.A. **74**:1635–1639.
27. **Williams, R. C., J. C. Gingrich, and A. N. Glazer.** 1980. Cyanobacterial phycobilisomes: particles from *Synechocystis* 6701 and two pigment mutants. J. Cell Biol. **85**:558–566.
28. **Yamanaka, G., A. N. Glazer, and R. C. Williams.** 1978. Cyanobacterial phycobilisomes. Characterization of the phycobilisomes of *Synechococcus* sp. 6301. J. Biol. Chem. **253**:8303–8310.
29. **Yu, M.-H., and A. N. Glazer.** 1982. Cyanobacterial phycobilisomes: role of the linker polypeptides in the assembly of phycocyanin. J. Biol. Chem. **257**:3429–3433.
30. **Yu, M.-H., A. N. Glazer, and R. C. Williams.** 1981. Cyanobacterial phycobilisomes: phycocyanin assembly in the rod substructures of *Anabaena variabilis* phycobilisomes. J. Biol. Chem. **256**:13130–13136.
31. **Zilinskas, B.** 1981. Phycobiliprotein complexes of the cyanophyte, *Nostoc* sp., p. 365–375. *In* G. Akoyunoglou (ed.), Photosynthesis III. Structure and molecular organization of the photosynthetic apparatus. Balaban International Science Services, Philadelphia, Pa.
32. **Zilinskas, B. A.** 1982. Isolation and characterization of the central component of the phycobilisome core of *Nostoc* sp. Plant Physiol. **70**:1060–1065.
33. **Zilinskas, B. A., and R. E. Glick.** 1981. Noncovalent intermolecular forces in phycobilisomes of *Porphyridium cruentum*. Plant Physiol. **68**:447–452.